Received: 3 August 2020 | Revised: 31 August 2020 | Accepted: 9 October 2020

DOI: 10.1002/jbt.22656

JOURNAL OF BIOCHEMICAL AND MOLECULAR TOXICOLOGY WILEY

# Discovery of novel pyrazole derivatives as a potent anti-inflammatory agent in RAW264.7 cells via inhibition of NF-κB for possible benefit against SARS-CoV-2

Anup Masih[1] | Amol K. Agnihotri[1] | Jitendra K. Srivastava[1] | Nidhi Pandey[2] | Hans R. Bhat[3] | Udaya P. Singh[1]

[1]Drug Design & Discovery Laboratory, Department of Pharmaceutical Sciences, Sam Higginbottom University of Agriculture, Technology & Sciences, Allahabad, Uttar Pradesh, India

[2]Department of Medicine and Health Sciences, University Rovira i Virgili, Tarragona, Spain

[3]Department of Pharmaceutical Sciences, Dibrugarh University, Dibrugarh, Assam, India

**Correspondence**
Udaya P. Singh, Drug Design & Discovery Laboratory, Department of Pharmaceutical Sciences, Sam Higginbottom University of Agriculture, Technology and Sciences, Allahabad 211007, Uttar Pradesh, India.
Email: udaysingh98@gmail.com and udaya.singh@shiats.edu.in

## Abstract

Due to unavailability of a specific drug/vaccine to attenuate severe acute respiratory syndrome coronavirus 2, the current strategy to combat the infection has been largely dependent upon the use of anti-inflammatory drugs to control cytokines storm responsible for respiratory depression. Thus, in this study, we discovered novel pyrazole analogs as a potent nuclear factor kappa B (NF-κB) inhibitor. The compounds were assessed for NF-κB transcriptional inhibitory activity in RAW264.7 cells after stimulation with lipopolysaccharides (LPS), revealing Compound **6c** as the most potent analog among the tested series. The effect of Compound **6c** was further investigated on the levels of interleukin-1β, tumor necrosis factor-α, and interleukin-6 in LPS-stimulated RAW267.4 cells by enzyme immunoassay, where it causes a significant reduction in the level of these cytokines. In Western blot analysis, Compound **6c** also causes the inhibition of inhibitor kappa B-α and NF-κB. It was found to be snugly fitted into the inner grove of the active site of NF-κB by forming H-bonds and a nonbonded interaction with Asn28 in a docking analysis.

**KEYWORDS**

docking, inflammation, NF-κB, pyrazole, SARS-CoV-2

## 1 | INTRODUCTION

The whole world is facing a severe unprecedented problem due to outbreak of coronavirus disease (COVID-19) caused by a positive-sense RNA virus. It is clinically termed as severe acute respiratory syndrome coronavirus 2 (SARS-CoV-2) and considered as an epidemic.[1,2] Till now, it has spread to more than 215 countries/territories, affected more than 10 million people, and responsible for death of more than 500,000 since it was first reported in late December 2019 in the Wuhan, China. Concerning the seriousness of situation and spreadability, on January 31, 2020, it was acknowledged as public health crisis for all the countries by World Health Organization.[3–5] Many of the people affected by the virus do not have serious clinical complications at an early stage of infection. However, some individuals report fever, cough or chest tightness, dysopnoea and, in some cases, mild/severe illness. Moreover, the patient suddenly progresses to the late stage of the infection, observing acute respiratory distress syndrome and multiple-organ failure, which result in death within a short time. Amassing confirmations propose that cytokine storm is the main reason underlying the severity and morbidity in COVID-19 patients, where immune cells were found highly active with production of massive inflammatory cytokines and chemical mediators.[6–9] SARS-CoV-2 after entering respiratory epithelial cells shows formation of a hyaline membrane and an increased infiltration of inflammatory cells with multinucleated syncytial cells.[10–12]

 © 2020 Wiley Periodicals LLC 

Studies have found an aberrant activation of nuclear factor kappa B (NF-κB) in inflammatory responses of SARS-CoV-2 infections.[13] It has a noteworthy part within the framework of immune system by acting as a key mediator of proinflammatory gene induction and facilitating cells belonging to both innate and adaptive immune system. It corresponds to the family of inducible transcription factors, which manages various genes that have been implicated in diverse processes of the immune and inflammatory responses. It was further subdivided into five fundamentally related individuals, for instance, NF-κB1 (or p50), NF-κB2 (or p52), RelA (or p65), RelB, and c-Rel, which induce transcription of intended genes by combining with a specific DNA facet.[14–17] The enactment of NF-κB may well be conceivable by the inclusion of two particular pathways, such as canonical and noncanonical (or another) pathways. Despite their contrasts in the signaling instrument, these both are considered vital for modulating immune and inflammatory responses.[18] The canonical NF-κB pathway could be activated by cytokines, growth factors, mitogens, microbial, and stress agents. Initially, it can be started by the inducible degradation of inhibitor kappa B-α (IκBα) stimulated by phosphorylation of a multisubunit IκB kinase (IKK) complex in a site-specific manner. The IKK is further subdivided into two catalytic subunits, IKK-α and IKK-β, and NF-κB essential modulator or IKK-γ, a regulatory subunit. Studies have shown that IKK could be easily activated by the action of mitogens, growth factors, stress agent cytokines, and microbial components.[19] Upon activation, the p50/RelA and p50/c-Rel dimers (canonical NF-κB member) get translocated from cytoplasm to nucleus through the phosphorylation of IκBα at two N-terminal serines, which is further ubiquitously degraded in proteosome.

However, the noncanonical NF-κB pathway is selectively stimulated to a certain cluster of inducers, such as ligands belonging to tumor necrosis factor (TNF) receptor superfamily members, for example, CD40, BAFFR, RANK, and LTβR.[16,20] Unlike the canonical pathway, it is not dependent on IκBα, but it may be dependent upon handling of the NF-κB2 forerunner protein (p100). Research has demonstrated the role of the canonical NF-κB pathway in nearly all areas of the immune response, whereas the noncanonical NF-κB pathway seems to be emerging as an external signaling axis operating together with the canonical NF-κB pathway to control the basic functions of the adaptive immune system.[21–23] There is currently no effective antiviral agent available to treat SARS-CoV-2 infection. Much attention is, therefore, focused on the regulation of cytokine storm and inflammatory reactions in SARS-CoV-2 infections, such as selective inhibition of NF-κB.

The current medicinal chemistry has been largely dependent on the heterocyclic compounds to develop newer drugs/agents due to ease of generating chemical diversity based on pharmacological or toxicological studies.[24] Pyrazole, a nitrogen-containing heterocyclic molecule, is found to possess numerous pharmacological activities.[25,26] It is also found in commercially successful drugs, such as celecoxib (anti-inflammatory), rimonabant (antiobesity), fomepizole (alcohol dehydrogenase inhibitor), and sildenafil (to improve erectile dysfunction). [26–28] Various recent studies have shown pyrazole as a potent inhibitor of NF-κB.[29] Moreover, we have also discovered some derivatives of pyrazoles as potent antibacterial [30] and anti-HIV-1 agents.[31,32] Therefore, in the present study, in continuation of our research activity on the development of small molecule inhibitors,[33–35] we intend to develop a novel series of pyrazole as a novel NF-κB inhibitor for possible benefit in SARS-CoV-2 infection.

## 2 | MATERIALS AND METHODS

### 2.1 | Chemistry

The synthesis of designed analogs has been achieved according to previously reported procedures.[36,37] The detailed procedure for synthesis, along with analytical spectroscopic data, has been provided in Supporting Information associated with the manuscript.

### 2.2 | Pharmacological activity

#### 2.2.1 | NF-κB transcriptional activity

The RAW264.7 macrophages (ATCC) were cultured in Dulbecco's modified Eagle's medium supplemented with 10% of FBS, 100 μg/ml of streptomycin, and 100 U/ml of penicillin in 5% $CO_2$ at 37°C. After attaining 80% confluency, the cells were transfected with 1 μg of the NF-κB reporter construct, alongside 0.5 μg of pSVGal plasmid, using Lipofect-AMINE 2000 (Invitrogen) in Opti-MEM medium (Gibco) and kept aside for 24 h. After transfection, the cells were treated with lipopolysaccharide (LPS) or dexamethasone (dex) and Compounds **6(a–g)** (10 μM) for an additional 2 h. The reporter lysis buffer (Promega) was used for lysing the cells. Also, 20 μl of cell extract and 100 μl of luciferin substrate (Promega) were used for the luciferase assay. The luciferase action was calculated using a Dual-Luciferase Reporter Assay System (Promega) as per the instruction provided by manufacturer. The data are normalized for transfection effectiveness by separating firefly luciferase action with that of Renilla luciferase.

#### 2.2.2 | TNF-α, interleukin-1β, and interleukin-6 assays

RAW264.7 cells ($5 \times 10^5$ cells/ml) after incubation for 16 h were pretreated with Compound **6c** (10, 20, and 50 μM) for 1 h, followed by stimulation by LPS (1 μg/ml). The enzyme-linked immunosorbent assay was performed to quantify the level of cytokines using supernatant obtained from the cell culture after 20 h of LPS stimulation.

#### 2.2.3 | Preparation of nuclear extracts

RAW264.7 cells were incubated for 10 min on ice after treating with lysis buffer. The resulting solution was centrifuged at 15,000*g* for 5 min

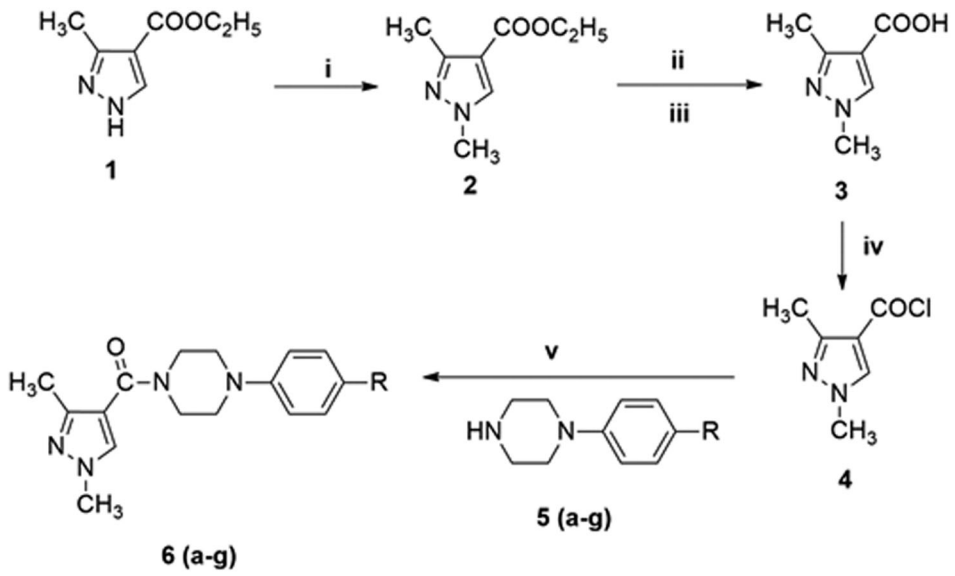


**SCHEME 1** The synthesis of target molecules. Reagent and conditions: (i) $(CH_3)_2SO_4$, DMF, 60°C, 3 h; (ii) NaOH, stirred; (iii) HCl, stirred, (iv) $SO_2Cl_2$, reflux, 4 h; (v) methylene dichloride, triethylamine, room temperature, 8–9 h

at 4°C, and the resulting pellet having raw nuclei was further suspended in extraction buffer (50 μl) and then incubated for further 30 min at 4°C on a shaker. The nuclear extract was obtained (supernatant) after centrifuging the above mixture for 10 min at 16,000*g*.

### 2.2.4 | Western blot analysis

RAW264.7 cells after incubation with Compound **6c** for 2 h were stimulated for 6 h with LPS (1 μg/ml). The cells than lysed with lysis buffer and allowed to centrifuge for 5 min at 12,000*g*. The resulting supernatant was obtained as total protein and the concentration was calculated using a protein assay kit. Furthermore, 10% sodium dodecyl sulfate–polyacrylamide gel electrophoresis was used to separate protein samples, which were further transferred on a polyvinylidene fluoride membrane (Millipore). To block the membrane in TBST, 5% skimmed milk was used. The resulting membrane was then treated with primary antibody (1:1000) and with respective secondary antibodies (1:5000; Cell Signaling Technology). The expressions of biomarkers were observed by enhanced chemiluminescence (Thermo Fischer Scientific Inc.) kit and ImageJ software was used to analyze the bands. Moreover, for determination of various biomarkers, the membrane was exposed using stripping buffer for 15 min on a shaker. The membrane was then washed with TBST and once more blocked with skimmed milk (5%) in TBST buffer. The membrane was then blotted with primary antibody (1:1000) and with respective secondary antibodies (1:5000).

**TABLE 1** Effect of pyrazole derivative 6(a–g) on NF-κB transcriptional activity in LPS-stimulated RAW264.7 cells[a]

| Compound | R | Relative NF-κB activity (NF-κB/TK, fold) |
|---|---|---|
| **6a** | 4-Cl | 2.12 ± 0.45[#] |
| **6b** | 4-Br | 2.78 ± 0.53[#] |
| **6c** | 4-F | 1.37 ± 0.12[#] |
| **6d** | 4-$CH_3$ | 4.05 ± 0.37[#] |
| **6e** | 4-$NO_2$ | 3.30 ± 0.65[#] |
| **6f** | 4-OH | 4.87 ± 1.02[#] |
| **6g** | 4-$OCH_3$ | 5.05 ± 1.31[#] |
| Dex (std) | | 1.20 ± 0.15[#] |
| Control | | 0.54 ± 0.05 |
| LPS | | 5.32 ± 0.56[**] |

Abbreviations: LPS, lipopolysaccharide; NF-κB, nuclear factor kappa B.
[a]$N = 3$.
[#]$p < .01$ versus LPS.
[**]$p < .01$ versus control.

### 2.2.5 | Molecular docking analysis

The docking study of the most active Compound **6c** was conducted using the CDOCKER protocol inbuilt in Discovery Studio 3.0 (DS 3.0; Dassault Systèmes BIOVIA, Discovery Studio Modeling Environment, Release 2018, San Diego, USA: Dassault Systèmes, 2016) with X-ray crystal structure of human $A_{2A}$ adenosine receptor cocrystallized with ligand ZM241385 at 2.6 Å resolution (PDB: 3EML). The protein model was downloaded from protein data bank. The binding pocket of human $A_{2A}$ adenosine receptor was defined using the inbuilt pdb coordinates of the three-dimensional (3D) structure. The water molecule and cocrystallized ligand were later removed, and the lost atom such as hydrogen

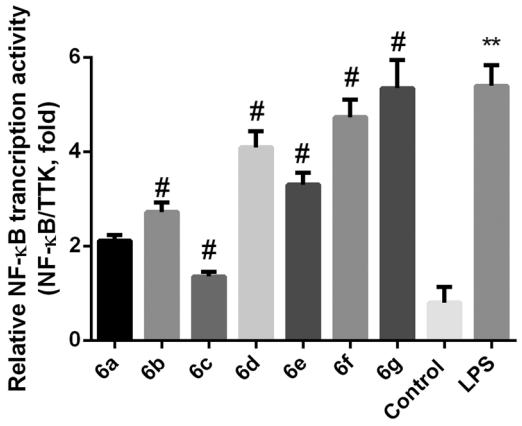


**FIGURE 1** Effect of Compound **6(a–g)** on the relative nuclear factor kappa B (NF-κB) transcription activity in lipopolysaccharide (LPS)-stimulated RAW264.7 cells. Results are the mean ± *SD* of three separate experiments. $^{**}p < .01$ is significant as compared with control-treated group; $^{\#}p < .01$ is significant as compared with LPS alone

was added to construct an initial receptor structure for docking. The docking was performed using the default parameters of the CDOCKER protocol. The receptor–ligand pose was visualized by the script feature of the DS 3.0 in both 2D and 3D formats.

## 3 | RESULT AND DISCUSSION

### 3.1 | Synthesis

The target derivatives were synthesized in excellent yield as outlined in Scheme 1. Initially, the synthesis was started with *N*-methylation of ethyl 3-methyl-1H-pyrazole-4-carboxylate (**1**) to afford ethyl 1,3-dimethyl-1H-pyrazole-4-carboxylate (**2**). The compound **2** was further proceed to ester hydrolysis under NaOH medium, and then by acidified with HCl to furnish Compound **3** (1,3-dimethyl-1H-pyrazole-4-carboxylic acid). The chlorination of Compound **3** with the help of $SO_2Cl_2$ afford 1,3-dimethyl-1H-pyrazole-4-carbonyl chloride (**4**). The target product **6(a–g)** was obtained by refluxing Compound **4** with the corresponding 4-substituted phenyl piperazine derivatives **5(a–g)** using triethylamine and methylene dichloride as solvent. The structures of Compounds **6(a–g)** was ascertained using Fourier-transform infrared (FT-IR), $^{1}$H nuclear magnetic resonance (NMR), $^{13}$C NMR, elemental and mass analysis. The Compound **6f** showed FT-IR stretching vibration at 3429 $cm^{-1}$ which corresponds to the aromatic OH group. Another peak at 3098–3089 $cm^{-1}$ suggested presence of aromatic C–H group linked to piperazine ring. The absorption band appeared at 2959–2959 $cm^{-1}$ confirms stretching vibration related to C–H of methyl group linked to pyrazole ring. An additional peak at 1282 $cm^{-1}$ appears due to aromatic $OCH_3$ group. The FT-IR peak at 1719–1715 $cm^{-1}$ showed stretching vibrations of C=O group. Absorption band at 1689–1682 $cm^{-1}$ corresponds to C=N group of pyrazole ring. Furthermore, the absorption band found at 1398–1391 $cm^{-1}$ and 1076–1063 $cm^{-1}$corresponds to of N–N of pyrazole ring and the C–N stretching vibrations, respectively. The $NO_2$ linked to aromatic phenyl appears at 1536 $cm^{-1}$. The stretching vibration 1154 $cm^{-1}$ suggested presence of aromatic fluoro group attached to piperazine ring. The presence of aromatic OH has been confirmed by a singlet peak at 9.42 ppm in entire title Compound **6(a–g)** in $^{1}$H NMR. The proton in the pyrazole ring showed as singlet at 8.72–8.71 due to presence of C–H group. Furthermore, the resonance at 8.01–6.96 ppm corresponds to C–H proton of aromatic ring as doublet, whereas one more proton in the phenyl ring appeared as doublet at 7.14–6.69 ppm. The aliphatic $CH_2$ proton appears at 3.64–3.10 ppm due to piperazine ring as multiplet. In addition, the singlet found at 3.69–3.67 ppm suggested the presence of $CH_3$ group linked to pyrazole ring. The proton in the $OCH_3$ group appeared as singlet as 2.34–2.31 ppm. In $^{13}$C NMR, the pyrazole ring carbon atom peaks appears at 146.9–112.4 ppm. The carbon of methyl group substituted at

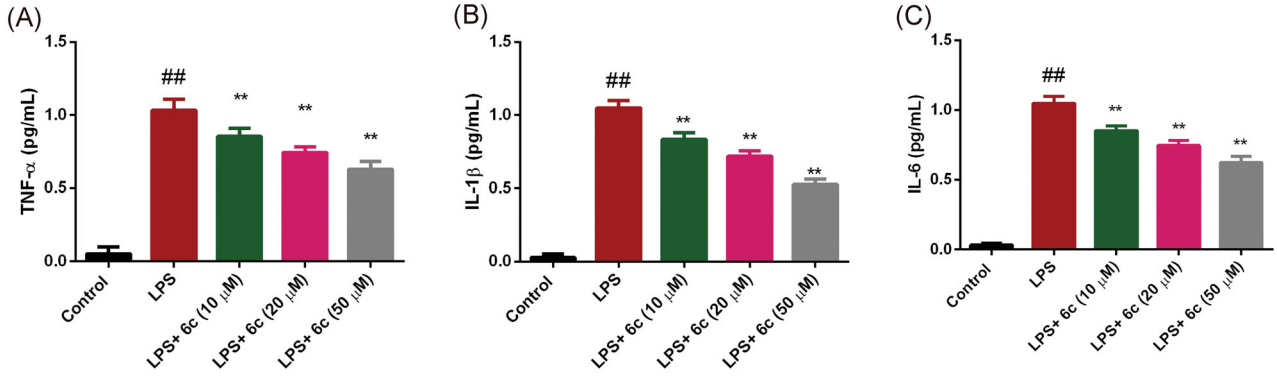


**FIGURE 2** Effect of Compound **6c** on the level of various proinflammatory cytokines in the RAW264.7 cells, where (A) tumor necrosis factor-α (TNF-α), (B) interleukin-1β (IL-1β), and (C) interleukin-6 (IL-6). Results are the mean ± *SD* of three separate experiments. $^{\#\#}p < .01$ is significant as compared with the control-treated group; $^{**}p < .01$ is significant as compared with lipopolysaccharide (LPS) alone

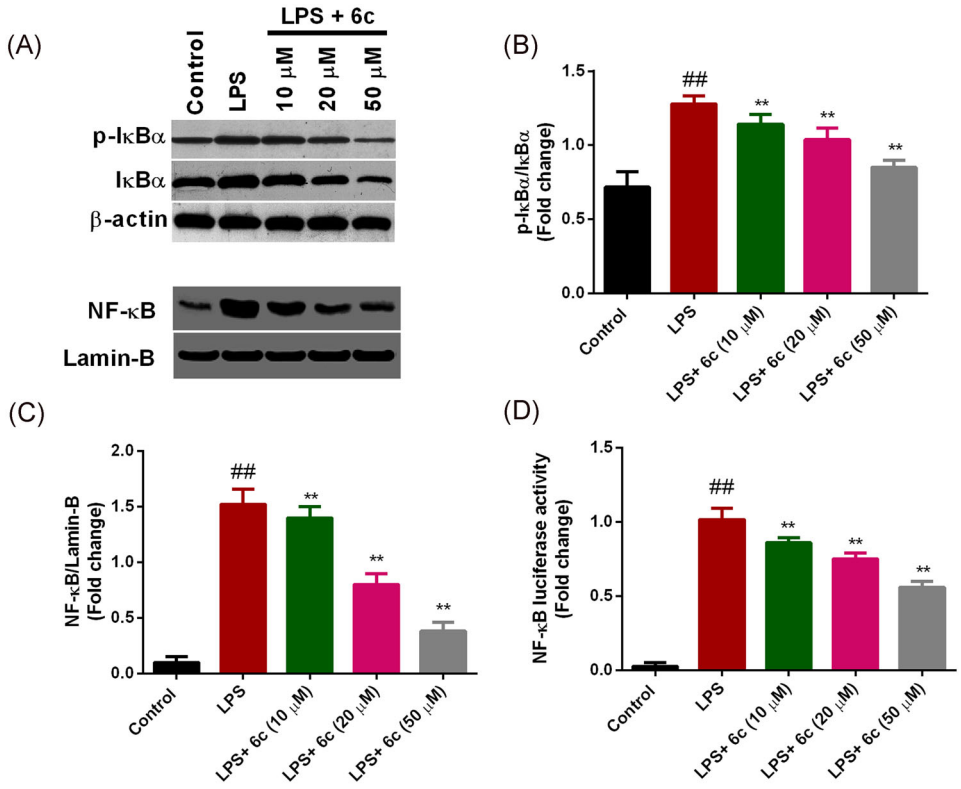


**FIGURE 3** Effect of Compound **6c** on nuclear factor kappa B (NF-κB) signaling cascade in lipopolysaccharide (LPS)-stimulated RAW264.7 cells by Western blot analysis, where (A) representative blots of p-IκBα (membrane was stripped and reprobed) and NF-κB, and corresponding bar graph of (B) p-IκBα and (C) NF-κB. (D) Effect of Compound **6c** in a diverse concentration on LPS-induced promoter activity of NF-κB in RAW264.7 cells. Results are the mean ± *SD* of three separate experiments. $^{\#\#}p < .01$ is significant as compared with the control-treated group; $^{**}p < .01$ is significant as compared with LPS alone. IκBα, inhibitor kappa B-α

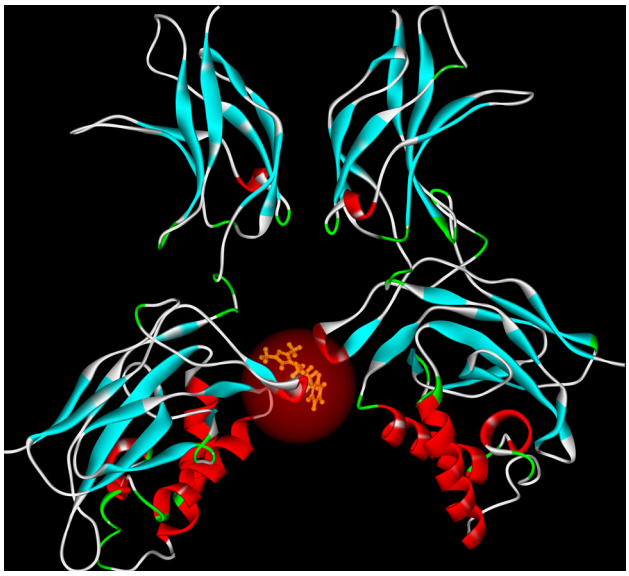

**FIGURE 4** Orientation of Compound **6c** in the active site (denoted by sphere in red) of nuclear factor kappa B (NF-κB; pdb: 1nfk)

pyrazole ring appeared at 40.1–13.4 ppm. Furthermore, the resonance peak appeared at 168.2 ppm corresponds to the carbon atom of carbonyl group. In addition, the resonance at 53.3–49.2 ppm attributed to the carbon of $CH_2$ of piperazine ring. Furthermore, the resonance at 149.5–114.3 ppm showed the presence of carbon of phenyl ring linked to piperazine ring. Finally, the mass spectroscopy and elemental analysis title Compounds **6(a–g)** corresponds to the structure of title compounds (Scheme 1).

## 3.2 | NF-κB inhibitory activity

In this study, a diverse series of novel pyrazoles was devised and synthesized, as shown in Scheme 1, toward finding a potent NF-κB inhibitor. The comparative inhibitory activity of target compounds is shown in Table 1. As presented in Table 1, Compound **6a** containing *p*-chloro showed a considerable inhibition of NF-κB transcription activity in LPS-stimulated RAW264.7 cells. The inhibitory activity was declined considerably in the case of Compound **6b**. The inhibitory potency was found highest among the tested series in

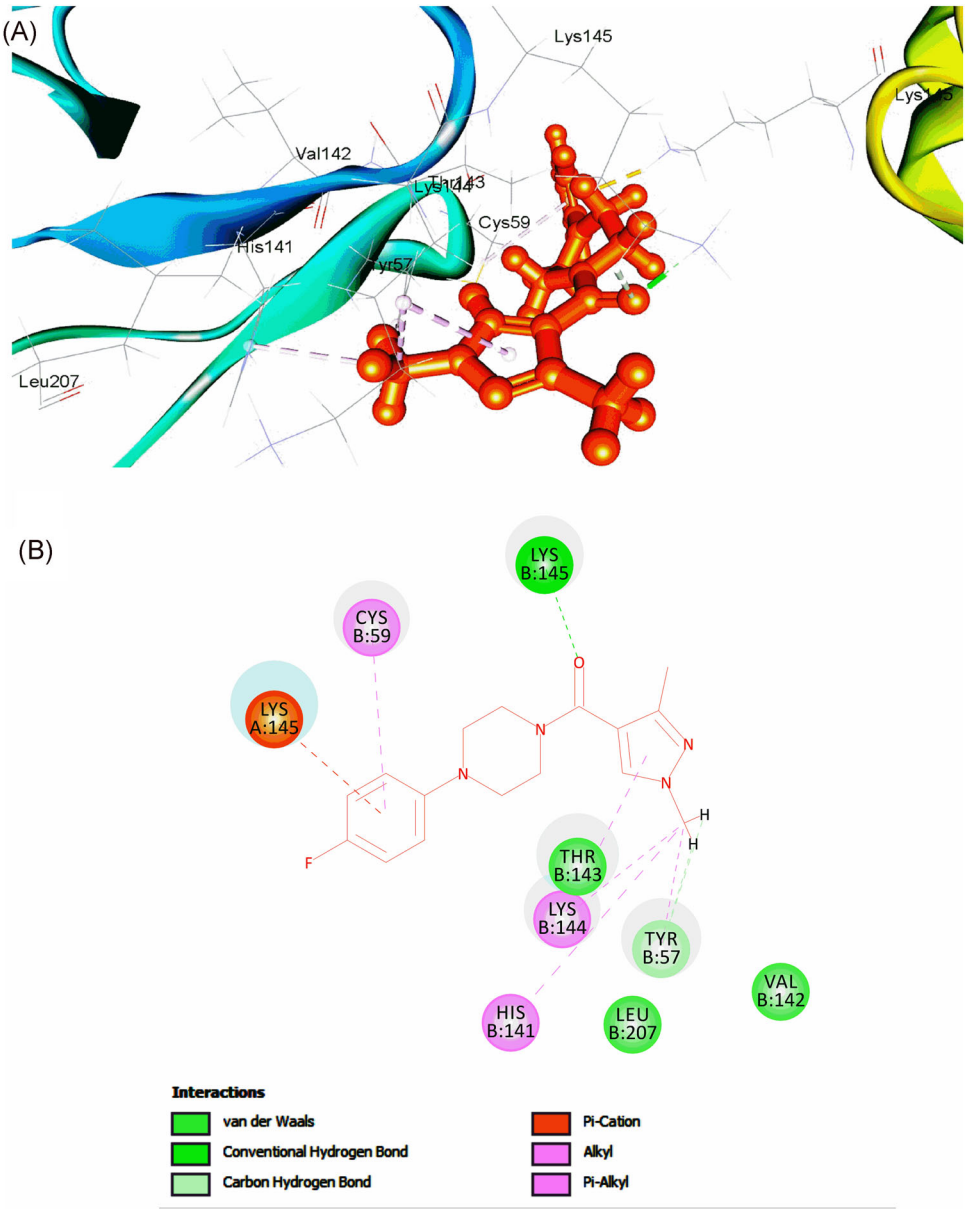


**FIGURE 5** Docked orientation of Compound **6c** in the active site of nuclear factor kappa B (NF-κB) depicting interactions (A) three-dimensional (3D) view and (B) 2D view with the neighboring residue (pdb: 1nfk)

the case of Compound **6c**. Upon replacement of fluoro with methyl (**6d**), the inhibitory potency was reduced significantly. However, with the insertion of the *p*-nitro group in the place of *p*-methyl (**6e**), the activity was improved moderately. The activity was further observed to be reduced in the case of Compounds **6f** and **6g** containing *p*-hydroxy and *p*-methoxy group, respectively. Moreover, none of the compounds showed a potent activity as compared with dexamethasone as a standard drug (Dex). As confirmed by the comparative effect of target derivatives (Figure 1), the structure–activity relationship studies suggested that compounds displayed a moderate-to-momentous inhibition of NF-κB transcription activity. On the basis of inhibitory potency, electron-withdrawing substituted derivatives displayed a significant inhibitory activity than their electron-donating counterparts.

### 3.3 | Effect on proinflammatory cytokines

Considering the importance of various proinflammatory cytokines in SARS-CoV-2 infections,[38,39] a enzyme immunoassay was conducted to investigate the inhibitory effect of most potent NF-κB inhibitor (Compound **6c**) on the levels of interleukin-1β, TNF-α, and interleukin-6 in LPS-stimulated RAW267.4 cells. As shown in Figure 2, LPS causes an increase in the concentration of studied cytokines in the culture supernatants of RAW264.7 cells in comparison to the control group. However, the level of the proinflammatory cytokines was found to be reduced significantly in a dose-dependent manner, with highest activity in the case of 50-μM concentration in the **6c**-treated group.

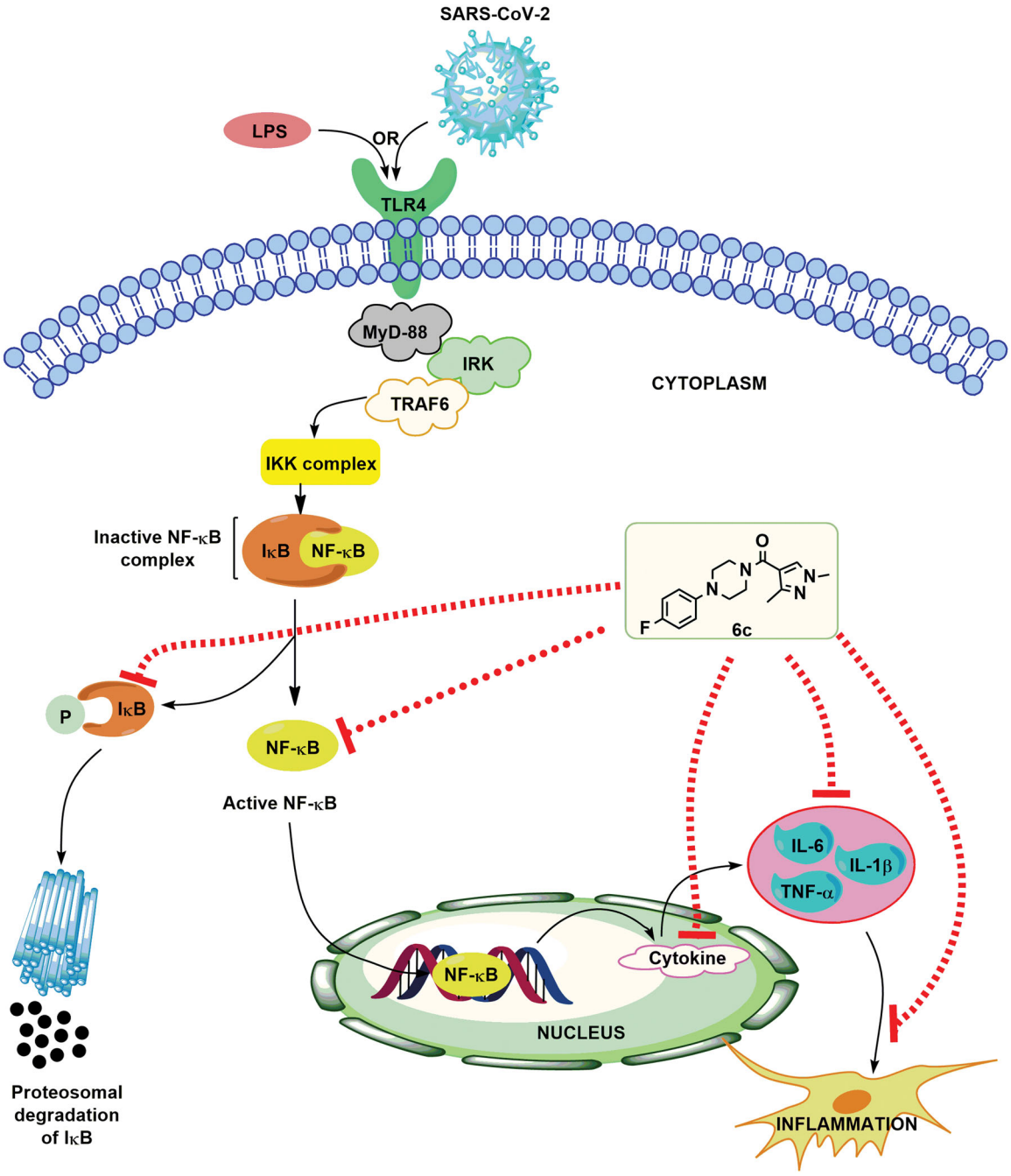


**FIGURE 6** A prospective mechanism of Compound **6c** as an anti-inflammatory agent. IKK, IκB kinase; IL-1β, interleukin-1β; IL-6, interleukin-6; IκBα, inhibitor kappa B-α; LPS, lipopolysaccharide; NF-κB, nuclear factor kappa B; SARS-CoV-2, severe acute respiratory syndrome coronavirus 2

### 3.4 | Effect of Compound 6c on the upstream mediators of the NF-κB signaling pathway

Various studies have implicated the role of NF-κB signaling cascade in the generation of various inflammatory cytokines in the LPS-stimulated macrophages.[40,41] Therefore, in this part of the study, we specifically investigate whether Compound **6c** could be competent enough to inhibit the activation of NF-κB signaling cascade and its upstream modulators, such as IκBα, by Western blot analysis. IκBα acts as a positive regulator to promote the activation of NF-κB signaling cascade after phosphorylation of IκB. As shown in Figure 3A,B, Compound **6c** causes a dose-dependent inhibition of p-IκBα in the cytosol as compared with the LPS group. The nuclear translocation of NF-κB is a critical step for the release of inflammatory cytokines; therefore, in this part, we intend to determine the effect of Compound **6c** on the nuclear translocation of NF-κB using nuclear extracts of LPS-stimulated RAW264.7 macrophages. As shown in Figure 3A,B, the

expression of NF-κB in the nucleus was found to be increased in the LPS group, as compared with control. Moreover, as expected, Compound **6c** causes a concentration-dependent inhibition of LPS-induced nuclear translocation of NF-κB. The observation was further found to be in accordance with the potent NF-κB inhibitory activity of Compound **6c**, as shown in Figure 1. Results of the study suggested that Compound **6c** causes the inhibition of release of various proinflammatory cytokines, possibly due to the inhibition of NF-κB activity.

## 3.5 | Molecular docking analysis

As presented in Figure 4, Compound **6c** was found to be deeply engulfed in the active site (as shown as red sphere) of the NF-κB protein model. Moreover, on close inspection, it was found that Compound **6c** efficiently interacted with neighboring residues via making various interatomic contacts. Compound **6c** formed one H-bond with Lys145 (Chain B) through a carbonyl oxygen atom. It also formed one π–cation interaction between phenyl linked to piperazine and Lys145 (Chain A). It was also observed to interact with Cys59, Thr153, Lys144, His141, and Tyr57 of Chain B in Figure 5. The results were further found in agreement with previous studies where potent NF-κB inhibitors interacted in a similar fashion.[42] On the basis of above studies, it is concluded that Compound **6c** can attenuate inflammatory cascade via inhibiting number of mediators, as depicted in Figure 6.

Collectively, in our present study, we have showed the development of novel pyrazole derivatives as a potent anti-inflammatory agent by inhibiting NF-κB activation in LPS-stimulated RAW264.7 cells. Results showed Compound **6c** as the most potent inhibitor of NF-κB transcription activity, which causes a significant inhibition of various proinflammtory cytokines, and a positive regulator of NF-κB activation (IκBα). Thus, Compound **6c** could be suggested as a potential lead for therapeutic application in controlling the inflammatory response in SARS-CoV-2 infection.

## ACKNOWLEDGMENT

All the authors are thankful to SHUATS for providing necessary infrastructural facilities.

## CONFLICT OF INTERESTS

The authors declare that there are no conflict of interests.

## AUTHOR CONTRIBUTIONS

Anup Masih contributed in the synthesis of molecules and wrote the original draft of the manuscript. Amol K. Agnihotri contributed in the synthesis of molecules and wrote the original draft of the manuscript. Jitendra K. Srivastava contributed in the pharmacological activity and wrote the original draft of the manuscript. Nidhi Pandey contributed in the pharmacological activity and wrote the original draft of the manuscript. Hans R. Bhat contributed in the docking study and wrote the original draft of the manuscript. Udaya P. Singh contributed in conceptualization and supervision of the study, and approved the final draft of the manuscript.

## ORCID

*Hans R. Bhat* http://orcid.org/0000-0002-9643-4916
*Udaya P. Singh* https://orcid.org/0000-0003-0865-0502

## REFERENCES

[1] T. P.Velavan, C. G. Meyer, *Trop. Med. Int. Health* **2020**, *25*, 278.
[2] A. Remuzzi, G. Remuzzi, *Lancet* **2020**, *395*, 1225.
[3] C. Sohrabi, Z. Alsafi, N. O'Neill, M. Khan, A. Kerwan, A. Al-Jabir, C. Iosifidis, R. Agha, *Int. J. Surg.* **2020**, *76*, 71.
[4] S. Kannan, P. Shaik Syed Ali, A. Sheeza, K. Hemalatha, *Eur. Rev. Med. Pharmacol. Sci.* **2020**, *24*, 2006.
[5] Y. C. Wu, C. S. Chen, Y. J. Chan, *J. Chin. Med. Assoc.* **2020**, *83*, 217.
[6] P. Mehta, D. F. McAuley, M. Brown, E. Sanchez, R. S. Tattersall, J. J. Manson, *Lancet* **2020**, *395*, 1033. https://doi.org/10.1016/S0140-6736(20)30628-0
[7] S. F. Pedersen, Y. C. Ho, *J. Clin. Invest.* **2020**, *130*, 2202.
[8] N. Vaninov, *Nat. Rev. Immunol.* **2020**, *20*, 277.
[9] Q. Ye, B. Wang, J. Mao, *J. Infect.* **2020**, *80*, 607.
[10] C. Chen, X. R. Zhang, Z. Y. Ju, W. F. He, *Zhonghua Shaoshang Zazhi* **2020**, *36*, 471.
[11] S. Felsenstein, J. A. Herbert, P. S. McNamara, C. M. Hedrich, *Clin. Immunol.* **2020**, *215*, 108448.
[12] X. Sun, T. Wang, D. Cai, Z. Hu, J. Chen, H. Liao, L. Zhi, H. Wei, Z. Zhang, Y. Qiu, J. Wang, A. Wang, *Cytokine Growth Factor Rev.* **2020**, *53*, 38.
[13] Y. R. Guo, Q. D. Cao, Z. S. Hong, Y. Y. Tan, S. D. Chen, H. J. Jin, K. Sen Tan, D. Y. Wang, Y. Yan, *Mil. Med. Res.* **2020**, *7*, 11.
[14] S. Ghosh, M. S. Hayden, *Nat. Rev. Immunol.* **2008**, *8*, 837.
[15] K. Newton, V. M. Dixit, *Cold Spring Harb. Perspect. Biol.* **2012**, *4*, a006049.
[16] T. Lawrence, *Cold Spring Harb. Perspect. Biol.* **2009**, *1*, a001651.
[17] T. Liu, L. Zhang, D. Joo, S.-C. Sun, *Signal Transduction Targeted Ther.* **2017**, *2*, 17023.
[18] S. C. Sun, *Nat. Rev. Immunol.* **2017**, *17*, 545.
[19] A. Rahman, F. Fazal, *Proc. Am. Thorac. Soc.* **2011**, *8*, 497.
[20] Y. Yamamoto, R. B. Gaynor, *J. Clin. Invest.* **2001**, *107*, 135.
[21] M. Neumann, M. Naumann, *FASEB J.* **2007**, *21*, 2642.
[22] R. E. Simmonds, B. M. Foxwell, *Rheumatology* **2008**, *47*, 584.
[23] P. P. Tak, G. S. Firestein, *J. Clin. Invest.* **2001**, *107*, 7.
[24] N. Kerru, L. Gummidi, S. Maddila, K. K. Gangu, S. B. Jonnalagadda, *Molecules* **2020**, *25*, 1909.
[25] A. Ansari, A. Ali, M. Asif, Shamsuzzaman, *New J. Chem.* **2017**, *41*, 16.
[26] J. V. Faria, P. F. Vegi, A. G. C. Miguita, M. S. dos Santos, N. Boechat, A. M. R. Bernardino, *Bioorg. Med. Chem.* **2017**, *25*, 5891.
[27] M. F. Khan, M. M. Alam, G. Verma, W. Akhtar, M. Akhter, M. Shaquiquzzaman, *Eur. J. Med. Chem.* **2016**, *120*, 170.
[28] M. Li, B. X. Zhao, *Eur. J. Med. Chem.* **2014**, *85*, 311.
[29] A. C. Pippione, S. Sainas, A. Federico, E. Lupino, M. Piccinini, M. Kubbutat, J. M. Contreras, C. Morice, A. Barge, A. Ducime, D. Boschi, S. Al-Karadaghi, M. L. Lolli, *MedChemComm* **2018**, *9*, 963.
[30] B. Singh, H. R. Bhat, M. K. Kumawat, U. P. Singh, *Bioorg. Med. Chem. Lett.* **2014**, *24*, 3321.
[31] U. P. Singh, H. R. Bhat, A. Verma, M. K. Kumawat, R. Kaur, S. K. Gupta, R. K. Singh, *RSC Adv.* **2013**, *3*, 17335.
[32] U. P. Singh, H. R. Bhat, *AIDS Res. Hum. Retroviruses* **2014**, *30*, A206.
[33] V. Dubey, M. Pathak, H. R. Bhat, U. P. Singh, *Chem. Biol. Drug Des.* **2012**, *80*, 598.
[34] S. Sahu, S. K. Ghosh, P. Gahtori, U. P. Singh, D. R. Bhattacharyya, H. R. Bhat, *Pharmacol. Rep.* **2019**, *71*, 762.

[35] J. K. Srivastava, G. G. Pillai, H. R. Bhat, A. Verma, U. P. Singh, *Sci. Rep.* **2017**, *7*, 5851.
[36] L. Qiao, P. P. Cai, Z. H. Shen, H. K. Wu, C. X. Tan, J. Q. Weng, X. H. Liu, *Heterocycl. Commun.* **2019**, *25*, 66.
[37] W. J. Si, X. B. Wang, M. Chen, M. Q. Wang, A. M. Lu, C. L. Yang, *New J. Chem.* **2019**, *43*, 3000.
[38] P. Sarzi-Puttini, V. Giorgi, S. Sirotti, D. Marotto, S. Ardizzone, G. Rizzardini, S. Antinori, M. Galli, *Clin. Exp. Rheumatol.* **2020**, *38*, 337.
[39] C. Liu, Q. Zhou, Y. Li, L. V. Garner, S. P. Watkins, L. J. Carter, J. Smoot, A. C. Gregg, A. D. Daniels, S. Jervey, D. Albaiu, *ACS Cent. Sci.* **2020**, *6*, 315.
[40] L. Fengyang, F. Yunhe, L. Bo, L. Zhicheng, L. Depeng, L. Dejie, Z. Wen, C. Yongguo, Z. Naisheng, Z. Xichen, Y. Zhengtao, *Inflammation* **2012**, *35*, 1669.
[41] X. Ying, K. Yu, X. Chen, H. Chen, J. Hong, S. Cheng, L. Peng, *Cell. Immunol.* **2013**, *285*, 49.
[42] J. K. Srivastava, N. T. Awatade, H. R. Bhat, A. Kmit, K. Mendes, M. Ramos, M. D. Amaral, U. P. Singh, *RSC Adv.* **2015**, *5*, 88710.

## SUPPORTING INFORMATION

Additional supporting information may be found online in the Supporting Information section.

**How to cite this article:** Masih A, Agnihotri AK, Srivastava JK, Pandey N, Bhat HR, Singh UP. Discovery of novel pyrazole derivatives as a potent anti-inflammatory agent in RAW264.7 cells via inhibition of NF-κB for possible benefit against SARS-CoV-2. *J Biochem Mol Toxicol*. 2021;35:e22656.
https://doi.org/10.1002/jbt.22656